Jiaqi LUO, Master Student
ricki62@163.com
School of Mathematics and Statistics, Guilin University of Technology, Guilin, China
Guangxi Colleges and Universities Key Laboratory of Applied Statistics, Guilin, China

Wei JI, PhD (corresponding author)
javeey@163.com
School of Mathematics and Statistics, Guilin University of Technology, Guilin, China
Guangxi Colleges and Universities Key Laboratory of Applied Statistics, Guilin, China

Dynamic Volatility Linkage between the Hong Kong and U.S. Stock Markets: Evidence from DCC-GARCH-Copula Models

Abstract. *Using daily returns on the Hang Seng Index and the S&P 500 from 1995 to 2025, this study investigates volatility dynamics and cross-market dependence between the U.S. equity market and Hong Kong as an offshore, China-exposed financial hub within a DCC–GARCH–Copula framework. EGARCH (1,1)-t delivers the best marginal fit, indicating asymmetric and fat-tailed volatility. In the dependence stage, information criteria favour the Plackett copula in both non-crisis and crisis subsamples. The DCC conditional correlation rises sharply and remains persistent during major stress episodes, notably around the Global Financial Crisis. Out-of-sample results indicate that forecasting performance is horizon- and market-specific: DCC is most accurate for short-horizon HSI volatility, BEKK is comparatively more robust at longer horizons, and GO-GARCH performs well for the S&P 500 across several settings. Overall, the research conclusion provides a reference for investors to mitigate cross-market risks; jointly modelling volatility and dependence provides a more reliable basis for state-contingent risk assessment and cross-border portfolio allocation.*

Keywords: *GARCH-Copula, stock market linkage, volatility spillovers, volatility forecasting, financial crisis.*

JEL Classification: C58, G15.

Received: 29 August 2025	Revised: 14 February 2026	Accepted: 4 March 2026

1. Introduction

With deepening global integration, cross-border equity linkages have strengthened, making international stock market interdependence central to both academic research and macro-prudential policy. As the largest and most influential financial market, the U.S. equity market – proxied by the S&P 500 – often serves as a global risk-pricing hub through which liquidity conditions, risk appetite, and information shocks propagate worldwide. In parallel, the Hong Kong market – represented by the Hang Seng Index (HSI) – is an exceptionally open financial centre

DOI: 10.24818/18423264/60.1.26.06

and a key offshore venue for China-related risk, linking mainland-exposed firms with global capital. Understanding volatility and dependence linkages between the S&P 500 and the HSI is therefore essential for characterising global-to-regional risk transmission through an internationally connected hub.

A central unresolved issue is whether sharp increases in cross-market dependence during turmoil reflect genuine contagion or simply stronger interdependence driven by shared shocks. This distinction determines whether diversification fails because the dependence structure itself shifts or because markets jointly react to common shocks under heightened volatility. It also shapes how policymakers interpret cross-border spillovers and how they design coordination mechanisms for crisis management and systemic risk surveillance.

Studies document significant co-movements and volatility spillovers between the U.S. market and China-related equity markets, including Hong Kong, particularly during stress episodes (Avdjiev et al., 2019; Yanting et al., 2023). Policy and geopolitical shocks – such as the Sino-U.S. trade war – amplify uncertainty and trigger cross-market repricing (Egger and Zhu, 2020), while spillovers are shown to be time-varying and event-driven (Ahmed, 2021; Xinyu & Zhengting, 2023). Methodologically, multivariate GARCH-family models capture conditional volatility and dynamic correlation, whereas Copula approaches characterise nonlinear dependence and tail co-movement beyond linear correlation (Xu et al., 2019; Fink et al., 2017; Lai & Hu, 2021). Evidence from major turmoil – including the 2008 Global Financial Crisis and COVID-19 – also points to strengthened dependence, consistent with "decoupling–recoupling" dynamics in U.S.–China financial linkages that may transmit to Hong Kong as an offshore China-exposed hub (Bekaert et al., 2022; Ge et al., 2022; Dooley & Hutchison, 2009). Despite these advances, inference on U.S.– Hong Kong linkages remains limited. Existing studies often rely on a single framework, reducing comparability of crisis dependence across volatility-based GARCH models and tail-sensitive Copulas under a unified estimation and diagnostic protocol. Many samples end before 2020, omitting the compounded effects of the trade conflict and COVID-19. Moreover, crisis mechanisms – herding, liquidity spirals, and policy spillovers – are rarely mapped to model-implied indicators (e.g., lower-tail dependence coefficient λ_L, asymmetry measures, or dependence-regime shifts), weakening economic interpretation.

This study responds to these gaps by combining volatility modelling and dependence modelling within a coherent empirical design for the S&P 500–HSI nexus. Marginal return dynamics are modelled using GARCH-family specifications that accommodate time-varying volatility and potential asymmetry, while cross-market dependence is captured using multiple Copula families, so that both linear co-movement and tail-specific dependence can be evaluated. Using daily data from 1995–2025 – covering the Global Financial Crisis, China-U.S. trade war, and the COVID-19 shock – the analysis compares dependence patterns across stress regimes and reduces the risk of conclusions driven by a short sample. Focusing on the United States–Hong Kong pair provides a direct setting to study global-to-regional transmission in an open financial hub. We hypothesise that the correlation between

the two markets strengthens and becomes highly persistent during crisis periods, whereas in non-crisis periods, the dependence structure is characterised by weak and approximately symmetric co-movement. Such evidence would be consistent with contagion, indicating a stress-state shift in the dependence structure. Our findings thus offer actionable insights for investors managing cross-market portfolios and for regulators designing early-warning systems for systemic risk.

The structure of this paper is organised as follows. Section 2 establishes the literature review and theoretical framework. Section 3 describes the data. Section 4 outlines the DCC-GARCH-Copula methodology. Section 5 discusses the main empirical results and forecasting performance. Section 6 concludes by presenting implications and directions for future research.

2. Literature Review and Theoretical Framework

2.1 Contagion Mechanisms and Their Empirical Implications

A central distinction in international financial linkages is between interdependence and contagion. Interdependence reflects co-movement driven by common fundamentals or global shocks and is consistent with rational information transmission across markets. Contagion denotes a crisis-induced increase in cross-market dependence that cannot be explained by shared fundamentals or time-varying volatility alone (Forbes et al., 2002; Kaminsky & Schmukler, 1999). This distinction matters because interdependence implies that diversification benefits remain broadly stable after controlling for systematic risk, whereas contagion implies an unstable dependence structure in stress periods, eroding diversification precisely when it is most needed (Bekaert et al., 2022; Ge et al., 2022).

Economic mechanisms yield testable implications for the form that contagion takes in the data. Herding and panic selling predict stronger synchronisation in joint downturns than in joint upswings, implying lower-tail dependence and dependence asymmetry (Longstaff, 2010; Yanting et al., 2023). Liquidity spirals and funding constraints (e.g., margin calls and balance-sheet tightening) imply state dependence, whereby dependence strengthens nonlinearly in high-volatility regimes (Bekaert et al., 2022). Policy and geopolitical shocks (e.g., trade-war announcements) can generate discrete shifts in dependence parameters rather than smooth evolution (Egger & Zhu, 2020; Ahmed, 2021; Gormsen & Koijen, 2020). These mechanisms motivate an empirical framework that moves beyond volatility-adjusted correlation to explicitly target tail asymmetry, nonlinearity, and structural breaks in dependence (Aloui et al., 2013; Xu et al., 2019; Fink et al., 2017).

The unique empirical characteristics of financial contagion generated by the above-mentioned mechanisms jointly justify the need for a modelling framework that captures time-varying, asymmetric, and tail-specific dependence.

2.2 A GARCH–Copula Framework for Identifying Contagion

Standard correlation measures are ill-suited for capturing crisis-driven linkages because financial returns exhibit non-normality, time-varying volatility, and dependence that concentrates in extreme outcomes. To address these features, a two-stage modelling approach is widely adopted. First, GARCH-family models are applied to each return series to capture volatility clustering and heavy tails, yielding standardised residuals that filter out predictable marginal dynamics. Second, copulas are employed to model the dependence structure of the probability integral transform (PIT)-transformed residuals, thereby describing the asymmetric tail characteristics.

This two-stage framework is well-suited to identifying the mechanisms described in Section 2.1, as it allows for flexible modelling of both volatility dynamics and asymmetric tail dependence. However, the GARCH–Copula approach faces practical challenges. Estimation may be computationally demanding and susceptible to over-parameterisation, and copula inference is sensitive to both the marginal specification and the chosen copula family. Elliptical copulas (Gaussian, Student-t) impose symmetric tail dependence and may understate the downside synchronisation typical of crises. To address these concerns, we adopt a robust identification strategy. Dependence is estimated from filtered innovations to separate shifts in co-movement from shifts in volatility, and results are compared across pre-defined crisis and tranquil subsamples to detect abnormal amplification. We evaluate multiple copula families – including asymmetric (Clayton, Gumbel) and rotated variants – to diagnose tail asymmetry. Finally, key findings are checked for robustness under alternative GARCH margins.

3. Data

The Hang Seng Index (HSI) of Hong Kong, China, a benchmark index covering ~50% of Hong Kong's total market capitalisation with over 60% weighting in Chinese-funded enterprises, serves as a critical link between mainland China and global capital markets. This index facilitates cross-border integration of the A-share market and accelerates financial market liberalisation, while also serving as a key barometer of China's economic development prospects. The Standard & Poor's 500 Index (S&P 500), comprising 500 leading U.S. publicly traded companies, is a primary gauge of U.S. economic performance and global market sentiment.

This study employs daily closing prices for the HSI and the S&P 500, sourced from the Wind database, covering the period from January 4, 1995, to May 21, 2025. We aligned the common trading days of the two sequences and obtained 5,560 observations. The sample spans several major episodes of financial stress, including the 1997 Asian Financial Crisis, the 2008 Global Financial Crisis, the U.S.–China trade conflict (2018–2020), and the COVID-19 pandemic, thereby facilitating an analysis of crisis-driven linkage dynamics. Daily log returns are computed using the continuous compounding method $r_{i,t} = 100\times(\ln p_{i,t} - \ln p_{i,t-1})$, we converted the

daily closing prices of both indices into log return series. Figure 1 shows the resulting return series for the HSI and S&P 500.

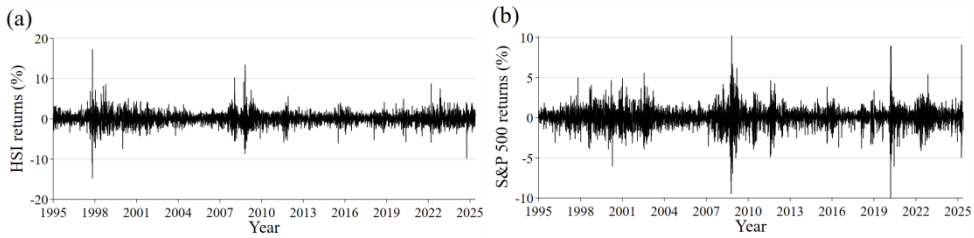

Figure 1. The time series plot of returns for the HSI and S&P 500
Note: (a) Daily log returns of HSI; (b) Daily log returns of S&P 500.
Source: Authors' own creation.

Figure 1 plots the daily log returns of the HSI and the S&P 500. Both series display pronounced volatility clustering and episodic spikes, indicating strong time variation in conditional variance and departures from normality. Large fluctuations are visible around major stress episodes, including the Asian financial crisis (1997-1998), the dot-com downturn (2000-2002), the global financial crisis (2008-2009), the Sino–U.S. trade conflict (2018-2020), and the COVID-19 shock (2020). The HSI exhibits particularly sharp movements during the Asian crisis, whereas the S&P 500 shows a relatively muted reaction in that episode, consistent with the perception that the initial impact of the crisis was more concentrated in emerging Asia at the time (Longstaff, 2010; Bekaert et al., 2022). In contrast, both markets show substantial volatility increases during the global financial crisis and the pandemic, reflecting periods of heightened global risk appetite and uncertainty (Gormsen & Koijen, 2020; Ge et al., 2022). Moreover, negative-return episodes tend to coincide with larger volatility bursts, which is consistent with leverage-type asymmetry documented in equity markets (Black, 1976; Nelson, 1991). These stylised facts motivate the use of heavy-tailed and asymmetric volatility models for the marginals and tail-sensitive dependence models for cross-market linkages (Engle, 2003; Aloui et al., 2013; Fink et al., 2017).

Table 1 reports descriptive statistics and diagnostic tests for the daily log returns of the HSI and the S&P 500. Both series exhibit substantial excess kurtosis (13.27 and 11.09, respectively), indicating leptokurtic distributions with fat tails, a finding confirmed by the highly significant Jarque–Bera test statistics at the 1% level. The ADF and PP unit-root tests strongly reject the null hypothesis for both series, confirming their stationarity. The Ljung–Box Q(10) statistics are significant, indicating the presence of serial correlation in the return series. The $Q^2(10)$ and ARCH-LM test results indicate that this serial correlation is mainly driven by conditional heteroskedasticity (i.e., volatility clustering) and leverage effects, rather than persistent mean dependence. These findings collectively provide strong empirical support for modelling the marginal return processes using heavy-tailed, asymmetric GARCH-type models to capture volatility clustering and leverage

effects, and for employing a multivariate framework that can account for time-varying cross-market dependence.

Table 1. Descriptive statistical table

	HSI	S&P 500
Mean	0.0201	0.0342
Std.Dev	1.5058	1.1648
Min	-14.7347	-9.9945
Max	17.2471	10.2457
Median	0.0284	0.0666
Skewness	0.2885	-0.0764
Kurtosis	13.2669	11.0938
Jarque-Bera	24496.7905***	15181.7259***
ADF	-63.7043***	-19.5698***
PP	-63.6968***	-68.5913***
Q(10)	27.4440***	29.5749***
$Q^2(10)$	1200.8425***	1676.8502***
ARCH	660.0802***	485.2179***

Note: ADF and PP denote the Augmented Dickey–Fuller and Phillips–Perron unit-root tests. Q(10) and Q²(10) are Ljung–Box statistics for returns and squared returns, respectively. ARCH denotes the ARCH-LM test. *** indicates significance at the 1% level.

Source: Authors' own creation.

4. Methodology

4.1 Model Specification

We employ the DCC-GARCH-Copula model to examine the volatility co-movement between the stock markets of Hong Kong, China, and the U.S., and to conduct volatility forecasting. We use the two-step estimation method proposed by Aloui et al. (2013). The GARCH model effectively captures volatility clustering, while the Copula model separates marginal distributions from joint distributions, allowing for the modelling of nonlinear dependencies.

Equity returns typically exhibit volatility clustering, with volatility surging and remaining elevated during episodes such as the 2008 Global Financial Crisis and the COVID-19 shock. The GARCH model captures this feature by linking conditional variance to past shocks and past variance. Compared to the normal distribution, stock index returns are characterised by leptokurtosis and heavy tails. Specifying the GARCH model residuals to follow a Student's t-distribution effectively captures such non-normal features. As a parsimonious and widely adopted specification, the GARCH(1,1) model is employed; thus, we estimate a GARCH(1,1)-t model for both the HSI and S&P 500 return series. The GARCH(p,q) model was originally proposed by Bollerslev (1986):

$$r_t=\mu_t+\varepsilon_t,\ \varepsilon_t=\sigma_t z_t,\ z_t \sim i.i.d\ (0,1) \quad (1)$$

$$\sigma_t^2=\omega+\sum_{i=1}^{q}\alpha_i\,\varepsilon_{t-i}^2+\sum_{j=1}^{p}\beta_j\,\sigma_{t-j}^2 \tag{2}$$

However, Black (1976) found that financial markets may show asymmetric volatility responses, where negative returns tends to generate more volatility than positive returns. The GARCH model imposes strict parameter constraints and cannot capture asymmetry, leading to systematic errors in volatility forecasts (Nelson, 1991). Thus, Nelson proposed the EGARCH model, which introduces an asymmetric volatility mechanism using the logarithm of conditional variance:

$$\ln(\sigma_t^2)=\omega+\sum_{\mathrm{i}=1}^{\mathrm{p}}\beta_i\ln(\sigma_{t-i}^2)+\sum_{\mathrm{j}=1}^{\mathrm{q}}\left[\alpha_j\left|\frac{\varepsilon_{t-j}}{\sigma_{t-j}}\right|+\gamma_j\frac{\varepsilon_{t-j}}{\sigma_{t-j}}\right] \tag{3}$$

Copula is a function that connects the marginal distributions of a multivariate distribution to its joint distribution (Nelsen, 2006). Sklar's theorem (1959), is the foundation of copula theory and establishes the relationship between multivariate distributions and copula functions. Suppose that the joint distribution function of the random vector $X=(X_1, \ldots, X_d)^{\mathrm{T}}$, d≥2 is $H(x)$, and the marginal distribution functions are $F_k(x_k)=\mathrm{P}(X_k\leq x_k)$(k=1, …, d). Then there exists a d-dimensional Copula function C: $[0, 1]^{\mathrm{d}}\rightarrow[0, 1]$ satisfying:

$$H(x_1, \ldots, x_d)=C(F_1(x_1), \ldots, F_d(x_d)) \tag{4}$$

$$h(x)=\left[\prod_{k=1}^{d}f_k(x_k)\right]\cdot c(F_1(x_1), \ldots, F_d(x_d)) \tag{5}$$

We use the standardised residuals from the EGARCH(1, 1)-t model as input and fit constant coefficient copula models.

The DCC-GARCH model is used to analyse dynamic correlations among multiple financial time series, forecast the conditional covariance matrix, and model volatility for multiple assets. We construct the DCC-GARCH(1, 1)-t model to analyse the dynamic correlation between the HSI and the S&P 500, assuming a multivariate Student's t-distribution to capture tail dependencies. We adopt the DCC-GARCH model proposed by Engle (2003). The DCC-GARCH(1, 1) model is specified as follows:

$$r_t=\mu_t+\epsilon_t,\ \epsilon_t|T_{t-1}\sim\mathrm{N}(0, H_t) \tag{6}$$

$$z_t=[z_{1,t}, z_{2,t}, \ldots, z_{N,t}]^{\mathrm{T}},\ \bar{Q}=\frac{1}{\mathrm{T}}\sum_{t=1}^{T}z_t\,z_t^{T} \tag{7}$$

$$Q_t=(1-\lambda_1-\lambda_2)\bar{Q}+\lambda_1 z_{t-1}z_{t-1}^{T}+\lambda_2 Q_{t-1} \tag{8}$$

Herein, λ_1 and λ_2 is required to satisfy $\lambda_1, \lambda_2\geq 0$ and $\lambda_1+\lambda_2<1$. The DCC matrix R_t and covariance matrix Q_t are as follows:

$$R_t=\mathrm{diag}(Q_t)^{-1/2}Q_t\mathrm{diag}(Q_t)^{-1/2} \tag{9}$$

$$H_t=D_tR_tD_t=\left(\rho_{ij,t}\sqrt{h_{ii,t}h_{jj,t}}\right),\ D_t=\mathrm{diag}(\sigma_{1,t}, \sigma_{2,t}, \ldots, \sigma_{N,t}) \tag{10}$$

4.2 Robustness Model

To assess the robustness of our results to the specification of multivariate conditional covariance dynamics, we re-estimate the volatility component using two widely adopted alternatives to DCC: BEKK-GARCH (Engle & Kroner, 1995) and GO-GARCH, while keeping the marginal filtering and copula-based dependence assessment unchanged. BEKK provides a parsimonious parameterisation that ensures the positive definiteness of the conditional covariance matrix H_t; the BEKK(1,1) specification is given by:

$$H_t = C'C + A'\varepsilon_{t-1}\varepsilon_{t-1}A + B'H_{t-1}B \quad (11)$$

where C, A, and B are parameter matrices. In our robustness check, we apply the BEKK model to the standardised innovations z_t obtained from the marginal EGARCH models. This "filtered BEKK" approach models the dynamic conditional covariance structure of the pre-whitened residuals, ensuring that any observed relationships are not merely artifacts of the marginal volatility filtering process.

As an additional robustness specification, we consider the Generalised Orthogonal GARCH (GO-GARCH) model of van der Weide (2002), which constructs multivariate volatility through a factor-based decomposition (Roy et al., 2022). The core idea is to represent the innovation vector as a linear combination of conditionally heteroskedastic but mutually uncorrelated latent factors:

$$\varepsilon_t = As_t, \qquad Var = (s_t|\mathcal{F}_{t-1}) = D_t \quad (12)$$

where A is a constant mixing matrix and D_t is diagonal, with each diagonal element following a univariate GARCH-type process. The conditional covariance matrix is therefore

$$H_t = AD_tA' \quad (13)$$

Following the standard GO-GARCH procedure, we extract latent factors via orthogonalisation or independent component analysis and fit univariate GARCH models to each factor to obtain their conditional variances.

5. Empirical Analysis

5.1 Estimation of Marginal GARCH Model

From 1995 to 2025, both the HSI and the S&P 500 experienced numerous short-term market shocks, strongly indicating conditional heteroskedasticity. Therefore, modelling and analysis using the GARCH family of models are theoretically and empirically justified.

Table 2 reports the estimation results for four volatility models: EGARCH(1, 1)-t, GJR-GARCH(1,1)-t, GARCH(1, 1)-t, and IGARCH(1, 1)-t. All models passed the ARCH-LM test ($p>0.05$), indicating no remaining conditional heteroskedasticity, and their standardised residuals showed white noise properties (Figure 2). This indicates that the models have effectively captured the conditional heteroskedasticity characteristics of the series, providing a reliable basis for subsequent volatility forecasts.

Table 2. Estimation Results of GARCH Models

	EGARCH(1, 1)-t		GJR-GARCH(1, 1)-t		GARCH(1, 1)-t		IGARCH(1, 1)-t	
	HSI	**S&P 500**	**HSI**	**S&P 500**	**HSI**	**S&P 500**	**HSI**	**S&P 500**
μ	0.0274	0.0609***	0.0302**	0.0627***	0.0436***	0.0820***	0.0441***	0.0822***
	(0.1287)	(<0.0001)	(0.0363)	(<0.0001)	(0.0022)	(<0.0001)	(0.0019)	(<0.0001)
AR(1)	-0.0130	-0.0386**	-0.0099	-0.0349**	-0.0101	-0.0406***	-0.0103	-0.0407***
	(0.6180)	(0.0161)	(0.4618)	(0.0113)	(0.4517)	(0.0034)	(0.4406)	(0.0033)
ω	0.0063***	-0.0065**	0.0183***	0.0222***	0.0155***	0.0193***	0.0105***	0.0179***
	(0.0002)	(0.0197)	(0.0009)	(<0.0001)	(0.0018)	(<0.0001)	(0.0002)	(<0.0001)
α_1	-0.0539***	-0.1250***	0.0296***	0.0285***	0.0621***	0.1382***	0.0659***	0.1418***
	(<0.0001)	(<0.0001)	(0.0002)	(0.0075)	(<0.0001)	(<0.0001)	(<0.0001)	(<0.0001)
β_1	0.9877***	0.9746***	0.9292***	0.8670***	0.9317***	0.8547***		
	(<0.0001)	(<0.0001)	(<0.0001)	(<0.0001)	(<0.0001)	(<0.0001)		
γ_1	0.1343***	0.1943***	0.1943***	0.1774***				
	(<0.0001)	(<0.0001)	(<0.0001)	(<0.0001)				
shape	6.9816***	6.2509***	7.0237***	6.3033***	6,8188***	5.9639***	6.3689***	5.8066***
	(<0.0001)	(<0.0001)	(<0.0001)	(<0.0001)	(<0.0001)	(<0.0001)	(<0.0001)	(<0.0001)

Note: *** indicates significance at the 1% level, and the values in parentheses represent the standard errors of the respective estimates.

Source: Authors' own creation.

Across all models, the *AR(1)* coefficients are negative for both markets, suggesting short-run negative autocorrelation in returns. The volatility dynamics are strongly supported by the data: in the symmetric models (GARCH and IGARCH), both indices exhibit high persistence, reflected in large and significant ARCH and GARCH terms; the IGARCH specification imposes unit persistence in variance ($\alpha+\beta=1$) by construction, implying long-lived volatility shocks. For asymmetric models, both EGARCH(1,1)-t and GJR-GARCH(1,1)-t yield statistically significant asymmetry (leverage) terms, indicating that negative shocks affect volatility differently from positive shocks in both the Hong Kong and U.S. markets. Moreover, the Student-t innovations are strongly favoured over the Gaussian benchmark, with estimated degrees of freedom indicating pronounced excess kurtosis and heavy tails. Overall, Table 2 shows that allowing for heavy tails and potential asymmetry is empirically important for modelling conditional volatility of the HSI and S&P 500, supporting subsequent dependence estimation based on filtered innovations and out-of-sample forecasting.

Table 3. The Comparative Results of the GARCH Models

index	EGARCH(1, 1)-t		GJR-GARCH(1, 1)-t		GARCH(1, 1)-t		IGARCH(1, 1)-t	
	HSI	S&P500	HSI	S&P500	HSI	S&P500	HSI	S&P500
Log-likelihood	**-9142.929**	**-7447.745**	-9143.814	-7459.369	-9165.082	-7510.575	-9167.092	-7510.84
RMSE	**1.504921**	**1.162462**	1.505109	1.162669	1.505249	1.163110	1.505245	1.163116
MAE	**1.035786**	**0.788494**	1.035878	0.788555	1.035928	0.788532	1.035926	0.788533
Akaike	**3.2913**	**2.6816**	3.2917	2.6857	3.2990	2.7038	3.2993	2.7035
Bayes	**3.2997**	**2.6899**	3.3000	2.6941	3.3061	2.7110	3.3053	2.7095
Hannan-Quinn	**3.2942**	**2.6845**	3.2946	2.6857	3.3014	2.7063	3.3014	2.7056

Note: This table reports log-likelihood (LL), RMSE, MAE, AIC, BIC, and HQIC values for the fitted models. Higher LL and lower RMSE, MAE, AIC, BIC, and HQIC values indicate better performance. Bold values denote the best-performing model for each metric.

Source: Authors' own creation.

To assess model fit, we use RMSE and MAE (lower values indicate higher accuracy) as accuracy measures and combine four goodness-of-fit indicators – Log-likelihood (higher values indicate better fit), AIC, BIC, and H-Q (smaller values indicate more concise models and better fit) – to select the best-performing GARCH model. The results of the model comparison are presented in Table 3. The EGARCH (1, 1)-t model outperforms others across all six evaluation indicators and better captures the volatility features of both indices. Therefore, we selected it as the best-fitting model and generated the standardised residual sequence based on this model (see Figure 2).

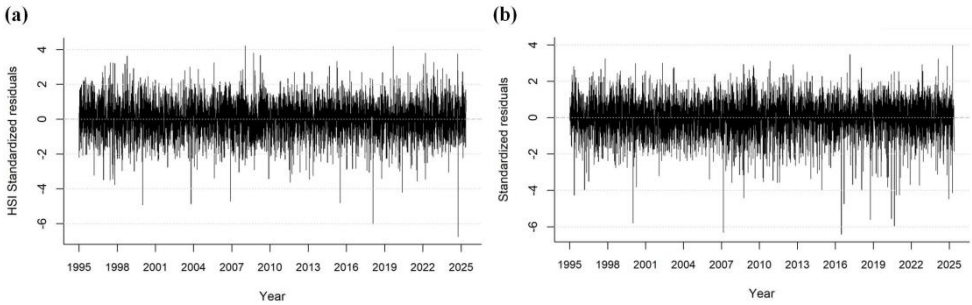

Figure 2. Standardised Residual Plot of HSI and S&P 500

Note: (a) Standardised residuals from the EGARCH(1,1)-t model fitted to the HSI; (b) Standardised residuals from the EGARCH(1,1)-t model fitted to the S&P 500.

Source: Authors' own creation.

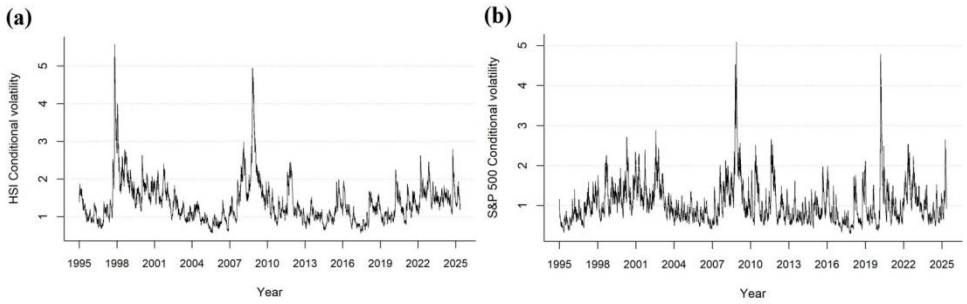

Figure 3. The conditional volatility plot of HSI and S&P 500

Note: (a) represents the conditional volatility generated from fitting the EGARCH(1,1)-t model to the HSI; (b) represents the same model to the S&P 500.

Source: Authors' own creation.

Based on the estimated parameters of the EGARCH(1,1)-t model and the actual return series, the conditional variance was generated recursively. The conditional volatility, defined as the square root of this variance, is plotted in Figure 3 for both indices.

Panel (a) shows that the HSI volatility spiked dramatically during the Asian Financial Crisis (1997-1998), reflecting the severe market turmoil in Hong Kong following Thailand's currency devaluation (Kaminsky et al., 1999). A second pronounced peak occurred in 2008, coinciding with the global financial crisis triggered by the U.S. subprime mortgage meltdown. Given Hong Kong's deep integration with global markets, its volatility surged significantly during this period. Panel (b) illustrates that S&P 500 volatility also exhibited sharp increases during these crises, particularly in 2008. Furthermore, a historic high in S&P 500 volatility was observed in early 2020, driven by unprecedented uncertainty surrounding the economic impact of the COVID-19 pandemic (Gormsen et al., 2020).

The time series of conditional volatility generated by the EGARCH(1,1)-t model demonstrates a strong correspondence with the timing and magnitude of these significant market shocks. This suggests that the model is capable of effectively capturing the dynamic evolution of volatility in response to major macroeconomic and financial events, thereby providing a reliable basis for subsequent analysis.

5.2 Fitting of Copula Models

After filtering the marginal mean-variance dynamics of HSI and S&P 500 with EGARCH(1,1)-t, we perform a PIT transformation on the standardised residuals to obtain pseudo-observations approximately following U(0,1), thereby isolating the identification of the dependence structure from marginal heteroskedasticity and fat tails. Table 4 reports the Copula fitting results for the non-crisis period (n = 4,921) and the crisis period (n = 639), including parameter estimates and standard errors, log-likelihood, AIC/BIC, tail dependence coefficients, and the K–S goodness-of-fit index.

Table 4. The fitting result of the copula model

Panel A: Non-Crisis Sub-period(n=4,921)

Copula	Parameters	Standard Error	Log-Likelihood	AIC	BIC	λ_L	λ_U	K-S
Plackett	***α*=1.54**	**0.0662**	**49.3**	**-98.5**	**-92.9**	**0**	**0**	**0.0202**
Frank	*α*=0.868	0.0876	49.1	-96.1	-89.6	0	0	0.0207
Gaussion	*α*=0.140	0.0141	46.5	-91.0	-84.5	0	0	0.0310
Student -t	*ρ*=0.142 *v=38.1*	0.0145 17.5	47.3	-90.7	-77.7	0.00003	0.00003	0.0530
Gumbel	*α*=1.09	0.0111	37.4	-72.9	-66.4	0	0.108	0.1520
Rotated Gumbel	*α*=1.07	0.00997	34.6	-67.1	-60.6	0.0912	0	0.0817
Rotated Clayton	*α*=0.207	0.0214	27.9	-53.8	-47.3	0	0.0351	0.1370
Clayton	*α*=0.207	0.0189	25.2	-48.4	-41.9	0.0351	0	0.0547

Panel B: Crisis Sub-period(n=639)

Copula	Parameters	Standard Error	Log-Likelihood	AIC	BIC	λ_L	λ_U	K-S
Plackett	***α*=2.01**	**0.218**	**19.4**	**-38.8**	**-34.3**	**0**	**0**	**0.0150**
Frank	*α*=1.39	0.226	19.0	-36.1	-31.6	0	0	0.0155
Gaussion	*α*=0.205	0.0327	18.0	-34.0	-29.6	0	0	0.0211
Student -t	*ρ*=0.212 *v=19.7*	0.0346 12.6	19.5	-34.9	-26.0	0.00147	0.00147	0.0265
Rotated Gumbel	*α*=1.12	0.0265	15.8	-29.6	-25.1	0.143	0	0.0240
Gumbel	*α*=1.14	0.0297	14.5	-27.0	-22.5	0	0.159	0.0537
Clayton	*α*=0.385	0.0516	7.74	-13.5	-9.01	0.166	0	0.0252
Rotated Clayton	*α*=0.385	0.0582	5.66	-9.32	-4.86	0	0.166	0.0701

Note: The bold values indicate the optimal model under each criterion.

Source: Authors' own creation.

Table 4 reports copula fits for HSI–S&P 500 dependence in the non-crisis (n = 4,921) and crisis (n = 639) subsamples using PIT-transformed innovations filtered by EGARCH(1,1)-t margins. Information criteria – especially BIC – consistently select the Plackett copula in both regimes, implying positive dependence beyond independence ($\alpha = 1$). The Plackett parameter increases from α=1.54 in the non-crisis

period to α=2.01 in the crisis period (about a 30% rise), indicating broad-based dependence tightening and reduced diversification benefits after marginal filtering. While the Plackett copula implies zero tail dependence, tail-sensitive specifications still suggest economically meaningful changes in extreme co-movement during crises (e.g., λ_L increases for rotated Gumbel and Clayton, and λ_U rises for Gumbel), consistent with intensified tail clustering under stress. However, these tail-dependent copulas yield inferior AIC/BIC relative to Plackett, suggesting that crisis dependence is primarily broad-based, with tail clustering as a secondary but non-negligible feature. Finally, the Plackett copula also exhibits relatively small Kolmogorov–Smirnov (K–S) distances in both subsamples, supporting its goodness-of-fit.

5.3 DCC-GARCH Model

We further analysed the dynamic correlation between HSI and S&P 500 using the DCC-GARCH(1, 1)-t model. Model fitting results are presented in Table 5.

Table 5. Estimation Results of the DCC-GARCH(1,1)-t Model

Panel A: Parameter estimates

	HSI	S&P 500
μ	0.028314 (0.173467)	0.060486*** (<0.0001)
ω	0.006270*** (0.000339)	-0.006463** (0.028054)
α_1	-0.054064*** (<0.0001)	-0.125632** (<0.0001)
β_1	0.987670*** (<0.0001)	0.974668*** (<0.0001)
γ_1	0.134525*** (<0.0001)	0.193995*** (<0.0001)
shape	6.965255*** (<0.0001)	6.252582*** (<0.0001)
$dcca_1$	0.001298 (0.230740)	
$dccb_1$	0.997642*** (<0.0001)	
mshape	7.698318*** (<0.0001)	

Panel B: Residual diagnostic tests

	HSI	S&P 500
Q(10)	10.643422 (0.3859647)	9.196477 (0.5135644)
$Q^2(10)$	40.208389*** (<0.0001)	8.943991 (0.5374272)
Jarque-Bera	656.649*** (<0.0001)	1454.700*** (<0.0001)
Mardia skewness	348.168*** (<0.0001)	
Mardia Kurtosis	39.275*** (<0.0001)	

Note: ***, ** indicate significance at the 1%, and 5% levels respectively. P values are in parentheses

Source: Authors' own creation.

Table 5 reports the estimation results of the DCC–GARCH(1, 1) model with Student's t innovations. In the mean equations, the intercept μ is positive for both markets and statistically significant for the S&P 500, indicating a statistically non-zero conditional mean component for the U.S. market. In the variance equations, volatility persistence is evident from the large magnitude of the EGARCH log-variance coefficient β_1 for the HSI and the S&P 500, implying slow decay of volatility shocks. Furthermore, the asymmetry term γ_1 is positive and highly significant for both series, which is consistent with leverage-type effects, whereby negative shocks are associated with stronger volatility responses. The estimated degrees of freedom (shape parameter) are finite and significant, supporting heavy-tailed innovations and motivating the Student's t specification for capturing extreme movements. Regarding the cross-market dependence, the DCC parameters imply highly persistent conditional correlations. Specifically, $dccb_1$ is close to unity, indicating that correlation dynamics are dominated by the long-run persistent component, whereas $dcca_1$ is extremely small and statistically insignificant, suggesting limited incremental contribution of short-run correlation shocks.

Panel B reports residual diagnostic tests. The Ljung–Box Q(10) statistics on standardised residuals are insignificant for both series, suggesting that the mean dynamics are adequately filtered. The Jarque–Bera and multivariate Mardia tests strongly reject normality, further supporting the relevance of fat-tailed innovations. Overall, the DCC–EGARCH–t model provides a coherent baseline for modelling time-varying volatility and correlation dynamics; the remaining $Q^2(10)$ evidence for the HSI motivates robustness checks using alternative multivariate volatility specifications. Accordingly, results from the BEKK-GARCH and GO-GARCH models are presented in the subsequent subsection.

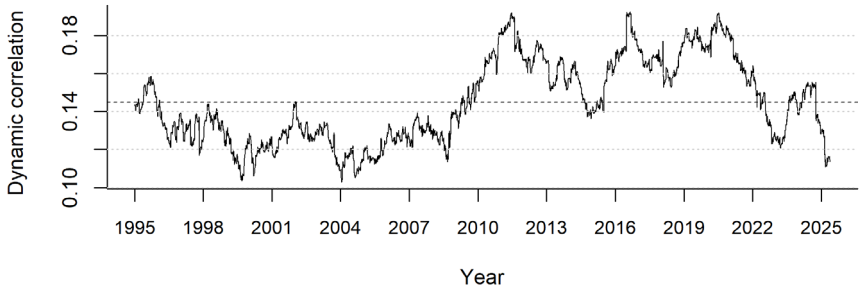

Figure 4. The dynamic correlation coefficient plot between HSI and S&P 500
Note: This figure presents the estimated dynamic conditional correlations of the DCC-GARCH(1, 1) model
Source: Authors' own creation.

Figure 4 plots the estimated dynamic conditional correlation (DCC) between the Hang Seng Index (HSI) and the S&P 500 from 1995 to 2025, derived from the DCC-GARCH(1,1) model. The dashed line represents the long-run mean correlation of approximately 0.14, indicating a persistent but moderate positive linkage. The DCC fluctuates around this level, confirming the time-varying comovement. Notably, the DCC rises above its mean during several periods of global financial stress. The late-1990s Asian financial crisis, the 2008-2009 Global Financial Crisis, and the 2018-2020 period marked by Sino-U.S. trade tensions and the COVID-19 shock all coincide with elevated correlations. This suggests that shared shocks and increased global uncertainty amplify cross-market synchronisation, reducing diversification benefits.

After the dot-com bubble burst in 2002, global market synchronisation led to an increase in the correlation between the two indices, both the Hong Kong and U.S. stock markets were impacted to some extent. This phenomenon is consistent with the cross-regional transmission of market sentiment (Pástor & Veronesi, 2005). In particular, the late-1990s Asian financial turmoil and the 2008–2009 global financial crisis coincide with relatively higher conditional correlations, suggesting that common risk factors and globally transmitted shocks are associated with increased cross-market comovement during stressed environments. The correlation is also comparatively elevated around 2018–2020, overlapping with intensified Sino–U.S. trade frictions and the COVID-19 shock. Importantly, because the DCC-GARCH framework primarily captures time-varying linear correlation dynamics, potential nonlinear dependence and tail comovement during crises are assessed jointly with the copula-based results and robustness checks reported in subsequent sections.

5.4 Robustness Model

To ensure robustness of the HSI-SP500 volatility co-movement findings, we employed BEKK-GARCH and GO-GARCH models as alternatives to the DCC-

GARCH-Copula framework. The GO-GARCH results (Table 6) show strong volatility persistence ($\beta > 0.7$) and smaller short-term shock impacts (α), confirming the persistent dynamic link found in the main analysis.

Table 6. Estimated Results of the GO-GARCH(1,1) Model

	Factor HSI	Factor S&P 500
omega	0.197034	0.003702
alpha	0.026446	0.001698
beta	0.775979	0.994626
Log-likelihood	-15680.6	

Note: GO-GARCH(1,1) factor volatility parameters (omega, alpha, beta) estimated on EGARCH(1,1)-t standardised innovations. Columns report latent orthogonal factors from the GO-GARCH decomposition.

Source: Authors' own creation.

Table 7. Estimated Parameters of the BEKK-GARCH Model

Parameter	Estimate	Std.Error
C[1,1]	0.308943**	0.142941
C[1,2]	0.653162	0.152472
C[2,1]	-	-
C[2,2]	0.743974***	0.134716
A[1,1]	0.017338	0.028560
A[1,2]	0.068122*	0.036702
A[2,1]	0.434904***	0.023176
A[2,2]	-0.004916	0.023015
B[1,1]	0.386019***	0.072062
B[1,2]	-0.116526	0.109175
B[2,1]	0.700618***	0.073501
B[2,2]	-0.007383	0.151919
Log-likelihood	-15590.2	

Note: 1. Matrices C, A, and B correspond to the constant, ARCH, and GARCH components of the BEKK variance equation, respectively. ***, **, and * denote statistical significance at the 1%, 5%, and 10% levels, respectively.

Source: Authors' own creation.

As shown in Table 7, the BEKK-GARCH model ensures the positive definiteness of the conditional covariance matrix. The significant cross-market term A[2,1] indicates a strong volatility spillover effect from the HSI to the S&P 500. The GARCH matrix B shows strong volatility persistence. These results confirm the persistent and asymmetric dynamic volatility linkages found in the DCC model, confirming the robustness of our main findings.

Table 8. Diagnostic Tests for the BEKK-GARCH and GO-GARCH Models

	GO-GARCH(1,1)		BEKK-GARCH(1,1)	
	HSI	**S&P 500**	**HSI**	**S&P 500**
Q(10)	10.643422 (0.385965)	9.196477 (0.513564)	10.833375 (0.370646)	15.449461 (0.116514)
$Q^2(10)$	40.2437*** (<0.0001)	9.002495 (0.531867)	34.779649*** (0.000136)	7.675884 (0.660462)
Jarque-Bera	656.649*** (<0.0001)	1454.700*** (<0.0001)	398.646*** (<0.0001)	1398.001*** (<0.0001)
Mradia-skewness	348.168*** (<0.0001)		321.612*** (<0.0001)	
Mradia-kurtosis	39.275*** (<0.0001)		35.614*** (<0.0001)	

Note:*** denote statistical significance at the 1% level. P values are in parentheses

Source: Authors' own creation.

Table 8 reports the residual diagnostic results of the BEKK-GARCH(1,1) and GO-GARCH(1,1) models as a robustness test. The Ljung–Box Q(10) tests for the standardised residuals of the two indices in both models are not significant, indicating that the serial correlation in the mean has been adequately eliminated. The $Q^2(10)$ statistic of the HSI remains significant under various multivariate settings, which reflects the stronger and more persistent second-moment dynamic characteristics inherent in the Hong Kong stock market. Compared to the S&P 500 Index, the Hang Seng Index is more susceptible to phased capital flows, policy interventions, and external shocks. These factors may generate complex, and long-memory volatility behaviours, which are difficult to completely eliminate even with a flexible multivariate GARCH structure. For both sequences, the Jarque-Bera test strongly rejected the normality assumption, and the multivariate Mardia skewness and kurtosis tests also rejected the joint normality, confirming significant non-Gaussian characteristics.

5.5 Volatility forecasting

To assess the volatility forecasting capabilities of different multivariate GARCH models, this chapter adopts a rolling out-of-sample prediction framework with a fixed estimation window. Specifically, the entire sample is divided into an in-sample estimation window and an out-of-sample prediction window: the last 500 trading days are used as the out-of-sample prediction period, and all previous observations are used as the initial estimation window. The prediction horizons include short-term (h = 1), medium-term (h = 5), and long-term (h = 20) levels.

Volatility forecasts are evaluated using the absolute daily return ($|r_t|$) as a proxy for realised volatility, with multi-horizon predictions assessed via h-day accumulated volatility$RV_{t,h} = \sum_{j=0}^{h-1} |r_{t+j}|$. Forecast accuracy is measured comprehensively by three metrics: Root Mean Squared Error (RMSE), Mean Absolute Error (MAE), and

the QLIKE loss function. QLIKE is robust to prediction errors on the variance scale and is the preferred loss function for volatility forecast evaluation (Patton, 2011).

Table 9. Out-of-Sample Volatility Forecast Performance of GARCH Models

Panel A: Hong Kong Stock Index (HSI)

Model comparison	RMSE			MAE			QLIKE		
	h = 1	h = 5	h = 20	h = 1	h = 5	h = 20	h = 1	h = 5	h = 20
DCC-GARCH	**1.1651**	3.1490	8.9763	**0.9271**	2.5495	8.0225	2.0134	4.8211	7.5216
BEKK-GARCH	1.1779	**3.1008**	**8.7522**	0.9311	**2.4819**	**7.7001**	2.0221	**4.8156**	**7.5126**
GO-GARCH	1.2075	3.4974	10.7644	0.9732	2.9360	9.7035	**2.0055**	4.8634	7.5740

Panel B: S&P 500 Index

Model comparison	RMSE			MAE			QLIKE		
	h = 1	h = 5	h = 20	h = 1	h = 5	h = 20	h = 1	h = 5	h = 20
DCC-GARCH	0.7803	2.0340	5.1901	0.5750	1.5457	4.7722	0.9718	3.8075	6.5250
BEKK-GARCH	0.7804	2.0177	5.1688	0.5759	1.5323	4.7624	**0.9714**	3.8036	6.5239
GO-GARCH	**0.7648**	**1.8830**	**4.1592**	**0.5558**	**1.3650**	**3.7717**	0.9761	**3.7659**	**6.4759**

Note: This table compares the out-of-sample forecast accuracy of DCC-GARCH, BEKK-GARCH, and GO-GARCH for HSI and S&P 500 volatility at horizons h = 1, 5, 20. Bold indicates the best model for each asset, horizon, and metric. Out-of-sample: 500 days.

Source: Authors' own creation.

Table 9 compares the out-of-sample forecast accuracy of DCC-GARCH, BEKK-GARCH, and GO-GARCH for HSI and S&P 500 volatility at horizons h = 1, 5, and 20. Bold entries indicate the best-performing model for each asset, horizon, and metric. For the volatility prediction of the HSI, both DCC-GARCH and BEKK-GARCH demonstrate comparable predictive accuracy across all time horizons, with no statistically significant differences in prediction errors. DCC is more suitable for short-term predictions, whereas BEKK is more appropriate for medium- and long-term predictions. In comparison, GO-GARCH consistently underperforms on all forecast horizons, indicating its limited suitability for this market. In the prediction of the S&P 500 index, the GO-GARCH model consistently delivers the best performance across all forecast horizons, indicating that its volatility persistence parameters are more aligned with the long-memory characteristics of mature markets. Overall, the selection of models for volatility prediction should fully take

into account the dual dimensions of market characteristics and the prediction horizon. The optimal model may vary for different markets and different horizons.

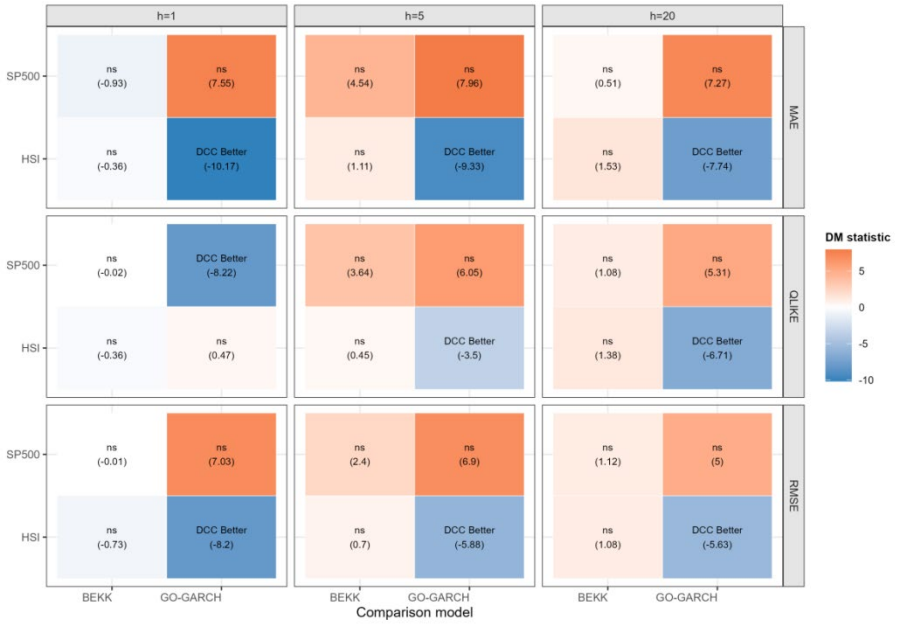

Figure 5. The significance map of the DM test for DCC vs BEKK/GO

Note: Negative values (blue cells) indicate that DCC yields lower prediction loss; positive values (red cells) indicate that the competing model yields lower prediction loss; and cells labelled "ns" denote statistical insignificance at the 10% significance level. The values in parentheses are the DM statistics.

Source: Authors' own creation.

Figure 5 presents a heat map of the Diebold–Mariano test results comparing DCC–GARCH with BEKK–GARCH and GO–GARCH across three forecast horizons (h=1, 5, 20) and three evaluation metrics (RMSE, MAE, QLIKE). The results shown in Figure 5 are in complete agreement with those of Table 9, indicating that the optimal predictive model can vary across forecast horizons and markets. There is no single multivariate volatility model that dominates across all assets, forecast horizons, and loss functions.

6. Conclusions and Outlook

This study applies a unified DCC–GARCH–Copula framework to characterise volatility dynamics and cross-market dependence between the S&P 500 and the HSI. On the marginal dimension, EGARCH(1,1)-t provides the best overall fit, indicating that volatility is asymmetric and return innovations exhibit fat tails, which makes flexible marginal filtering essential before dependence inference. On the dependence dimension, model comparison suggests that the Plackett copula delivers the best

overall fit by information criteria, and tail-sensitive specifications still indicate economically non-negligible downside clustering during crisis periods, implying that crisis co-movement is strengthened both through higher general dependence and through elevated joint downside risk. Consistent with this, DCC conditional correlations rise and remain persistent during major shocks, suggesting that cross-market linkages intensify under stress and can take time to normalise. Out-of-sample evidence further shows that no single multivariate volatility model dominates across assets, horizons, and loss functions: DCC performs better for short-horizon HSI forecasts, BEKK is comparatively more robust at longer horizons, and GO-GARCH performs well for the S&P 500 across several settings. These findings support horizon- and objective-specific model choice (or forecast combinations) in practical risk systems.

For regulatory authorities, systemic risk monitoring should not rely solely on static correlation coefficients, but should incorporate a "dual-layered early warning framework" simultaneously considering dynamic correlations and tail dependence indicators. Stress testing scenarios should employ state-dependent dependence structures to avoid overestimating diversification benefits. In terms of investment practice, a monitoring mechanism should be established to identify whether the market is switching from a "low volatility/low correlation" range to a "high volatility/high correlation" range. Once a switching signal is detected, the overall portfolio's risk exposure should be proactively reduced. For the public, this study underscores that the risk of synchronous market declines globally rises significantly during crises, highlighting the necessity for enhanced risk disclosure and investor education to prevent the misinterpretation of normal-period correlations as a safeguard during turbulent times.

Future research can be extended in three directions. First, time-varying or regime-switching Copula models (e.g., Markov-switching dependence structures) can be introduced to capture continuous changes in tail dependence over time and to more rigorously distinguish contagion from interdependence. Second, exogenous variables – such as the VIX, global liquidity, policy uncertainty, or geopolitical risk – can be embedded into the parameter equations of the DCC or Copula models, enabling testable mappings between economic mechanisms and dependence parameters. Third, the analysis can be extended from volatility forecasting to tail risk prediction and economic value assessment (e.g., back testing of ES and CoVaR, portfolio utility, and drawdown control), and further combined with realised volatility or expanded to multi-market networks and vine Copulas, so as to examine broader cross-market risk transmission mechanisms.

Acknowledgements: *This work was supported by the National Natural Science Foundation of China (Grant No. 12561083).*

References

[1] Aloui, R., Aïssa, M.S.B., Nguyen, D.K. (2013), *Conditional dependence structure between oil prices and exchange rates: A copula-GARCH approach. Journal of International Money and Finance*, 32, 719-738.

[2] Avdjiev, S.V., Bruno, C. Koch, H., Shin, S. (2019), *The Dollar Exchange Rate as a Global Risk Factor: Evidence from Investment. IMF Economic Review*, 67(1), 151-173.

[3] Ahmed, R. (2021), *Monetary policy spillovers under intermediate exchange rate regimes. Journal of International Money and Finance*, 112, 102342.

[4] Black, F. (1976), *Studies of Stock Price Volatility Changes. Proceedings of the 1976 meetings of the business & economics statistics section, american statistical association*, 81, 177-181.

[5] Bollerslev, T. (1986), *Generalized autoregressive conditional heteroskedasticity. Eeri Research Paper*, 31(3), 307-327.

[6] Bekaert, G., Engstrom, E.C., Xu, N.R. (2022), *The time variation in risk appetite and uncertainty. Management Science*, 68(6), 3975-4004.

[7] Dooley, M., Hutchison, M. (2009), *Transmission of the U.S. subprime crisis to emerging markets: Evidence on the decoupling–recoupling hypothesis. Journal of International Money and Finance*, 28(8), 1331-1349.

[8] Engle, R.F. (2003), *Dynamic Conditional Correlation: A Simple Class of Multivariate Generalized Autoregressive Conditional Heteroskedasticity Models. Journal of Business & Economic Statistics*, 20(3), 339-350.

[9] Engle, R.F., Kroner, K.F. (1995), *Multivariate simultaneous generalized ARCH. Econometric theory*, 11(1), 122-150.

[10] Egger, P.H., Zhu, J. (2020), *The US-Chinese trade war: An event study of stock-market responses. Economic Policy*, 35(103), 519-559.

[11] Fink, H., Klimova, Y., Czado, C., Stöber, J. (2017), *Regime switching vine copula models for global equity and volatility indices. Econometrics*, 5(1), 3.

[12] Forbes, K.J., Rigobon, R. (2002), *No contagion, only interdependence: measuring stock market comovements. The journal of Finance*, 57(5), 2223-2261.

[13] Ge, S., Zhiqing, X., Farhan, B.M., Ali, S.S.M. (2022), *Co-movement dynamics of US and Chinese stock market: evidence from COVID-19 crisis. Economic Research-Ekonomska Istraživanja*, 35(1), 2460-2476.

[14] Gormsen, N.J., Koijen, R.S. (2020), *Coronavirus: Impact on stock prices and growth expectations. The Review of Asset Pricing Studies*, 10(4), 574-597.

[15] Kaminsky, G.L., Schmukler, S.L. (1999), *What triggers market jitters? A chronicle of the Asian crisis. Journal of international money and finance*, 18(4), 537-560.

[16] Kaminsky, G.L., Reinhart, C.M. (1999), *The twin crises: the causes of banking and balance-of-payments problems. American economic review*, 89(3), 473-500.

[17] Lai, Y., Hu, Y. (2021), *Study on Tail Characteristics of Systemic Risk in US and Chinese Stock Markets. 2nd International Conference on Economic Development and Innovation (EDI 2021), Hong Kong, China.*

[18] Longstaff, F.A. (2010), *The subprime credit crisis and contagion in financial markets. Journal of Financial Economics*, 97(3), 436-450.

[19] Nelson, D.B. (1991), *Conditional heteroskedasticity in asset returns: A new approach. Econometrica: Journal of the econometric society*, 347-370.

[20] Nelsen, R.B. (2006), *An Introduction to Copulas.* Springer, New York, NY, USA.

[21] Pástor, Ľ., Veronesi, P. (2005), *Was there a Nasdaq bubble in the late 1990s? Journal of Financial Economics*, 81(1), 61-100.

[22] Patton, A.J. (2011), *Volatility forecast comparison using imperfect volatility proxies. Journal of econometrics*, 160(1), 246-256.

[23] Sklar, M. (1959), *Fonctions de répartition à n dimensions et leurs marges. In Annales de l'ISUP*, 8(3), 229-231.

[24] van der Weide, R. (2002), *Go-GARCH: A multivariate generalized orthogonal GARCH model. Journal of Applied Econometrics,* 17(5), 549-564.

[25] Xinyu, W., Zhengting, J. (2023), *Time-varying asymmetric volatility spillovers among China's carbon markets, new energy market and stock market under the shocks of major events. Energy Economics*, 126, 107004.

[26] Xu, W., Ma, F., Chen, W., Zhang, B. (2019), *Asymmetric volatility spillovers between oil and stock markets: Evidence from China and the United States. Energy Economics*, 80, 310-320.

[27] Yanting, Z., Xin, L., Xin, L., Jiaming, L. (2023), *A new view of risk contagion by decomposition of dependence structure: Empirical analysis of Sino-US stock markets. International Review of Financial Analysis*, 90, 102920.